

Thermal Quantum correlation in a three qubit spin chain under an inhomogeneous magnetic field

Matin Alipour

Department of physics, University of Chicago

Abstract

In this paper, we have investigated the thermal quantum correlation of a three-qubit spin of XY type in an inhomogeneity magnetic field, and The concurrency criterion is used to measure the degree of entanglement between two neighboring qubits. Also, the dependence of the thermal interweaving on the variable parameters of the magnetic field \mathcal{B} , temperature T and the amount of inhomogeneity of the magnetic field b has been investigated. and the discord-like quantifiers, namely the trace distance discord are computed. The results using the concurrency criterion show that thermal quantum entanglement decreases with the increase of all three parameters \mathcal{B} , T and b . In addition, by changing and controlling the mentioned parameters, it is possible to control the thermal entanglement between non-adjacent spins, $c(\rho_{13})$, and increase its value to a greater amount than the thermal entanglement between adjacent spins, $c(\rho_{12})$ and $c(\rho_{23})$ reached. Finally, the temperature variation of thermal entanglement between spins has been compared with the time variation of peer entanglement and also the results using Trace distance discord behaves similar to concurrence and has a decreasing trend with increasing, and $\mathcal{D}_T^{(13)}(\rho)$ has a lower value than $\mathcal{D}_T^{(12)}(\rho)$ and $\mathcal{D}_T^{(23)}(\rho)$ and can be increased.

Keywords: thermal quantum correlation, thermal quantum entanglement, spin chain, inhomogeneity magnetic field, concurrency, trace distance discord

1 Introduction

Through EPR)Einstein-Podolsky-Rosen (correlation, we can transfer an unaltered quantum state from one place to another (or the so-called teleportation) by a sender who does not know how far away the receiver is and information does not have [1]. In classical physics, it does not disturb the measurement of the system, but in quantum physics, the opposite of this statement is true and this disturbance can be used to measure quantum correlation, it can be said that some separable states still have quantum correlation and the result of this Quantum correlation is more general than entanglement [2].

Quantum entanglement was first stated by Schrödinger, which emphasizes the inherent order of statistical relationships between complex quantum subsystems [3]. Quantum entanglement is a very surprising feature in quantum mechanics, a kind of inherent non-local correlation, which is considered as a very important factor for quantum information and computing, and is used in dense coding and remote transmission of information compression or quantum states [4]. Also, in the conducted studies, it can be claimed that quantum mechanics protects cryptography according to the issue of key distribution [5]. If we want to have a definition of entanglement for the pair system, then the net entanglement of a quantum pair system is formed in the form of entropy for each member of the system [4].

In quantum systems, what is important for us in quantum information theory is to specify and quantitatively process information given by entanglement [6]. Quantum entanglement,

which has been studied a lot in these years, needs a theory in order to quantify it and according to it, we can control it and observe its changes [7].

Quantum entanglement can be based on scaling theory, also there are many differences between non-local and classical quantum correlation and entanglement, and a total correlation can be separated into two quantum and classical correlations [8,9].

One of the criteria that is used to measure entanglement is concurrence, which can be used to examine different models, and in the examination using this criterion, we can control the entanglement and using the existing parameter He observed its changes in the quantum system [10].

It should be kept in mind that external factors affect quantum entanglement. Also, chaos of quantum system like spin chain can reduce entanglement [11].

According to the mentioned points, the creation of a maximum entangled state for a two-qubit system that is far from each other can be used to transfer a one-qubit state about which we have no information with high fidelity from one side to the other [12].

One of the things that is investigated in the articles is thermal entanglement, and investigations in a two-qubit system show that various parameters and their control can increase thermal entanglement and bring it to the maximum value, such as the coupling constant, Temperature and magnetic field [13,14,15].

Another idea is to create a constant or heterogeneous magnetic field that can affect the entanglement and we can control it and use it for different models of a quantum system. If we consider the magnetic field to be inhomogeneous, for a quantum system including spin, we can see that in ferromagnetism, a lot of thermal entanglement can be created with low inhomogeneity [16,17,18,19,20].

Entanglement has uses that can be expressed, in entanglement it is used to understand the properties of solid state systems. This correlation is very important in the solid state systems which is manifested in the spin chain, and also the entanglement in the diamond structure can be checked in the XXZ model and it can be seen that different parameters such as the temperature of the magnetic field are effective [21,22]. In examining entanglement for ferromagnetic and antiferromagnetic materials, both of which have this property [23]. By using the electron spins in the semiconductor quantum dots that are coupled, we prepare quantum gates, which provide the desired entanglement [24].

Quantum discord was presented by Ollivier and Zurek . It is a measure of quantum entanglement and is not limited to entanglement and can be a measure of quantum correlation [6,25,26,27]. If we want to have a definition for trace distance discord, trace discord is actually a measurement of the difference between two natural quantum analogs and different from classical mutual information and can be used to determine their entanglement and uncertainty [2,28,29]. Quantum discord is a kind of quantum correlation which is defined according to the difference between quantum and classical mutual information. Also, to measure the distance of our desired state, the closest quantum-classical state is used [30,31]. For the geometric expression of quantum correlation, three cases are introduced, which are: the geometric discord, the measurement induced geometric discord, and the discord of response, each of which is defined based on three contraction distances in the set of quantum states, which are the tracking distances of Bursa and It expresses Hillenger [32]. Also, the

investigations carried out show that Quantum Discord cannot be the reason for its behind its speedup [33]. Also, there are different methods to calculate quantum correlation and in a spin system this correlation has been investigated using quantum discord and there are also different types of dependence such as magnetic field which can change and control it [34,35,36].

The non-equilibrium thermal entanglement in the quantum discord in the thermal bath has been investigated for different temperatures and it is possible that the temperature difference plays an important role in the correlation[38].

What we can add to the desired quantum system is Dzyaloshinski–Moriya (DM), which is observed to be a better channel for long-distance transport in the ferromagnetic spin chain. And this also makes a quantum system including different spins affected and changed, you can observe it and control it, and different models can be investigated using it [39,40,41].

In this article, a three-qubit spin chain in an inhomogeneous magnetic field has been investigated to measure quantum correlation using concurrency and trace discord distance. In fact, the spin chain is one of the candidates for the construction of quantum computers, where coding and Heisenberg interaction can be used in quantum calculations. Also, one of the important challenges of the quantum computer is the issue of entanglement.

2 Concurrency and trace distance discord

There are various indices to measure quantum correlation, which we have examined quantum entanglement and trace distance discord. In this paper, we have introduced the inhomogeneous magnetic field and investigated its effects on the quantum correlation between adjacent and non-adjacent spins in the chain. For this purpose, we have first calculated the Hamiltonian spectrum of the system and obtained the reduced density matrix for the relevant subsystems. Then, through concurrency and trace distance discord for X states, we have calculated quantum correlation, two-qubit subsystems, and we will continue to introduce the model and details of the problem.

The concurrency for the two-qubit system, which is used as a quantum entanglement criterion, is defined as follows[7]:

$$c(\rho) = \max\{0, \lambda_1 - \lambda_2 - \lambda_3 - \lambda_4\} \quad (1)$$

where ρ is the density matrix of the system and The values of λ_i ($i = 1, 2, 3, 4$) are the roots of the eigenvalues of the following operator :

$$R = (\sigma_1^Y \otimes \sigma_2^Y) \rho^* (\sigma_1^Y \otimes \sigma_2^Y)^\dagger \quad (2)$$

ρ^* is the complex conjugate of the density matrix.

For X -type two-qubit states whose density matrix is as follows:

$$\rho = \begin{pmatrix} \rho^{11} & 0 & 0 & \rho^{14} \\ 0 & \rho^{22} & \rho^{23} & 0 \\ 0 & \rho^{32} & \rho^{33} & 0 \\ \rho^{41} & 0 & 0 & \rho^{44} \end{pmatrix} \quad (3)$$

Concurrence is derived from equation (1) as follows :

$$c(\rho) = 2\max\{0, |\rho^{23}| - \sqrt{\rho^{11}\rho^{44}}, |\rho^{14}| - \sqrt{\rho^{22}\rho^{33}}\} \quad (4)$$

The next approach to calculate quantum correlation is trace distance discord. It is a reliable geometric quantifier of discord-like correlations.

The discord trace between the density matrix ρ_{AB} and ρ_{CD} is as follows[42]:

$$\mathcal{D}_T(\rho_{AB}) = \min_{\rho_{CD} \in \delta} \|\rho_{AB} - \rho_{CD}\| \quad (5)$$

where δ is the set of classical quantum states with vanishing quantum discord and $\|\tau\| = \text{Tr}(\sqrt{\tau^\dagger \tau})$ defines the trace norm of a generic operator τ .

$R_{\mu\nu}$ are the components of the correlation matrix are obtained from the Fano-Bloch decomposition of the density matrix ρ' [43].

$$\rho' = \frac{1}{4} \sum_{\mu, \nu=0}^3 R_{\mu\nu} \sigma_\mu \otimes \sigma_\nu \quad (6)$$

where $R_{\mu\nu} = \text{Tr}(\rho' \sigma_\mu \otimes \sigma_\nu)$ and in the equation above ρ' is

$$\rho \rightarrow \rho' = \begin{pmatrix} \rho^{11} & 0 & 0 & |\rho^{14}| \\ 0 & \rho^{22} & |\rho^{23}| & 0 \\ 0 & |\rho^{32}| & \rho^{33} & 0 \\ |\rho^{41}| & 0 & 0 & \rho^{44} \end{pmatrix} \quad (7)$$

The non vanishing components $R_{\mu\nu}$ are

$$\begin{cases} R_{00} = \text{Tr}(\rho) = 1, & R_{30} = 1 - 2(\rho_{33} + \rho_{44}), & R_{11} = 2(|\rho_{23}| - |\rho_{14}|) \\ R_{33} = 1 - 2(\rho_{22} + \rho_{33}), & R_{03} = 1 - 2(\rho_{22} + \rho_{44}), & R_{22} = 2(|\rho_{23}| + |\rho_{14}|) \end{cases} \quad (8)$$

The discord trace distance for the two- qubit state is expressed as follows[31]:

$$\mathcal{D}_T(\rho) = \sqrt{\frac{R_{11}^2 R_{max}^2 - R_{22}^2 R_{min}^2}{R_{max}^2 - R_{min}^2 + R_{11}^2 - R_{22}^2}} \quad (9)$$

$$R_{max}^2 \equiv \max\{R_{33}^2, R_{22}^2 + R_{30}^2\}, \quad R_{min}^2 = \min\{R_{11}^2, R_{33}^2\} \quad (10)$$

3 XY Heisenberg model for three-qubit spin chain

In this section, we study the three-qubit Heisenberg model, which is under the influence of inhomogeneity magnetic field. This model is given by the following Hamiltonian[14,16]

$$\mathcal{H} = \mathcal{J}(\sigma_1^X \sigma_2^X + \sigma_2^X \sigma_3^X + \sigma_1^Y \sigma_2^Y + \sigma_2^Y \sigma_3^Y) + \mathcal{B}_1 \sigma_1^Z + \mathcal{B}_2 \sigma_2^Z + \mathcal{B}_3 \sigma_3^Z \quad (11)$$

Using the Jordan-Wigner transformation, the above Hamiltonian can be written as follows:

$$\mathcal{H} = 2\mathcal{J}(\sigma_1^+ \sigma_2^- + \sigma_2^+ \sigma_3^- + \sigma_1^- \sigma_2^+ + \sigma_2^- \sigma_3^+) + \mathcal{B}_1 \sigma_1^Z + \mathcal{B}_2 \sigma_2^Z + \mathcal{B}_3 \sigma_3^Z \quad (12)$$

In equation (11), $\sigma_n = (\sigma_n^X, \sigma_n^Y, \sigma_n^Z)$ are the Pauli matrices and the index n is the number of the qubit, which varies from 1 to 3. \mathcal{B} is the magnetic field in the Z direction. \mathcal{J} is the coupling constant, if the coupling constant is $\mathcal{J} < 0$, it is related to the ferromagnetic chain, and if $\mathcal{J} > 0$, it is to the antiferromagnetic chain. For simplicity, we will consider $\mathcal{J} = 1$ in our calculations. We consider the local magnetic fields on the qubits as follows

$$\mathcal{B}_1 = \mathcal{B} + b, \quad \mathcal{B}_2 = \mathcal{B}, \quad \mathcal{B}_3 = \mathcal{B} - b \quad (13)$$

In the above equations, b is the magnetic field inhomogeneity parameter.

By choosing the calculation base as follows,

$$\{|000\rangle, |001\rangle, |010\rangle, |100\rangle, |110\rangle, |101\rangle, |011\rangle, |111\rangle\}$$

The Hamiltonian eigenvalues are as follows

$$\begin{cases} E_1 = 3\mathcal{B}, & E_2 = \mathcal{B} + 2\Delta, & E_3 = \mathcal{B}, & E_4 = \mathcal{B} - 2\Delta \\ E_5 = -\mathcal{B} - 2\Delta, & E_6 = -\mathcal{B}, & E_7 = -\mathcal{B} + 2\Delta, & E_8 = -3\mathcal{B} \end{cases} \quad (14)$$

The eigenvectors are as follows

$$\begin{cases} |\psi_1\rangle = |000\rangle \\ |\psi_2\rangle = \frac{1}{\Delta(\Delta + b)} [(\Delta^2 + b\Delta - 1)|001\rangle + (\Delta + b)|010\rangle + |100\rangle] \\ |\psi_3\rangle = \frac{1}{\Delta} (-|001\rangle + b|010\rangle + |100\rangle) \\ |\psi_4\rangle = \frac{1}{\Delta(\Delta - b)} [(\Delta^2 - b\Delta - 1)|001\rangle + (\Delta - b)|010\rangle + |100\rangle] \\ |\psi_5\rangle = \frac{1}{\Delta(\Delta - b)} [(\Delta^2 - b\Delta - 1)|011\rangle + (\Delta - b)|101\rangle + |110\rangle] \\ |\psi_6\rangle = \frac{1}{\Delta} (-|011\rangle + b|101\rangle + |110\rangle) \\ |\psi_7\rangle = \frac{1}{\Delta(\Delta + b)} [(\Delta^2 + b\Delta - 1)|011\rangle + (\Delta + b)|101\rangle + |110\rangle] \\ |\psi_8\rangle = |111\rangle \end{cases} \quad (15)$$

In the equations (14) and (15), Δ is defined as

$$\Delta = \sqrt{2 + b^2}$$

In the following section, I will discuss the states of two-qubit subsystems and thermal entanglement, such as them and trace distance discord.

4 Thermal quantum entanglement of subsystems

4.1 Reduced density matrices for two-qubit subsystems

To investigate thermal quantum entanglement between adjacent and non-adjacent qubits in the studied three-spin chain, we need to calculate reduced density matrices. Fortunately, the states of the two-qubit subsystems are all X-type, and their intersection can be accurately calculated through equation (4).

In thermal equilibrium, the state of the system at temperature T can be described by the following density matrix:

$$\rho(T) = \frac{1}{Z} \exp[-\beta\mathcal{H}] = \frac{1}{Z} \sum_{n=1}^8 \exp[-\beta E_n] |\psi_n\rangle \langle \psi_n| \quad (16)$$

In the above relation, $\beta = 1/K_B T$ and K_B is Boltzmann's constant. Z is the scattering function of the system, which is given by the relation $Z = \text{Tr}(\exp(-\beta\mathcal{H}))$. Using the Hamiltonian partition function in the previous section, the Z partition function is calculated as follows:

$$Z = 2\cosh(3\beta\mathcal{B}) + 2\cosh(\beta\mathcal{B}) + 4\cosh(\beta\mathcal{B})\cosh(2\beta\Delta) \quad (17)$$

Now, using (16), the density matrix is found and the reduced density matrices related to adjacent qubits (neighbor) and non-adjacent qubits, $\rho^{(12)}(T)$, $\rho^{(13)}(T)$ and $\rho^{(23)}(T)$ using partial tracking $\rho^{(12)}(T) = \text{Tr}_3(\rho(T))$, $\rho^{(13)}(T) = \text{Tr}_2(\rho(T))$ and $\rho^{(23)}(T) = \text{Tr}_1(\rho(T))$ Then we will investigate the intersection between qubits.

$$\left\{ \begin{array}{l} \rho_{11}^{(12)}(T) = e^{(-\beta\mathcal{B})} [e^{(-2\beta\mathcal{B})} + (\frac{1}{\Delta})^2 + \Omega^2 e^{(-2\beta\Delta)} + \Phi^2 e^{(2\beta\Delta)}] \\ \rho_{22}^{(12)}(T) = (\frac{1}{\Delta})^2 (b^2 e^{(\beta\mathcal{B})} + e^{(-\beta\mathcal{B})}) + \Omega^2 e^{(-2\beta\Delta)} (\theta^2 e^{(-\beta\mathcal{B})} + e^{(\beta\mathcal{B})}) + \Phi^2 e^{(2\beta\Delta)} (\Theta^2 e^{(-\beta\mathcal{B})} + e^{(\beta\mathcal{B})}) \\ \rho_{23}^{(12)}(T) = 2(\frac{1}{\Delta})^2 b \sinh(\beta\mathcal{B}) + \xi \Omega^2 e^{(-2\beta\Delta)} (\theta e^{(-\beta\mathcal{B})} + e^{(\beta\mathcal{B})}) + \gamma \Phi^2 e^{(2\beta\Delta)} (\Theta e^{(-\beta\mathcal{B})} + e^{(\beta\mathcal{B})}) \\ \rho_{32}^{(12)}(T) = 2(\frac{1}{\Delta})^2 b \sinh(\beta\mathcal{B}) + \xi \Omega^2 e^{(-2\beta\Delta)} (\theta e^{(-\beta\mathcal{B})} + e^{(\beta\mathcal{B})}) + \gamma \Phi^2 e^{(2\beta\Delta)} (\Theta e^{(-\beta\mathcal{B})} + e^{(\beta\mathcal{B})}) \\ \rho_{33}^{(12)}(T) = (\frac{1}{\Delta})^2 (b^2 e^{(-\beta\mathcal{B})} + e^{(\beta\mathcal{B})}) + \Omega^2 e^{(-2\beta\Delta)} (\xi^2 e^{(-\beta\mathcal{B})} + e^{(\beta\mathcal{B})}) + \Phi^2 \gamma e^{(2\beta\Delta)} (\Theta e^{(-\beta\mathcal{B})} + e^{(\beta\mathcal{B})}) \\ \rho_{44}^{(12)}(T) = e^{(\beta\mathcal{B})} [e^{(2\beta\mathcal{B})} + (\frac{1}{\Delta})^2 + \theta^2 \Omega^2 e^{(-2\beta\Delta)} + \Theta^2 \Phi^2 e^{(2\beta\Delta)}] \end{array} \right. \quad (18)$$

In equations (18), we have used the following notation:

$$\begin{cases} \Omega = \frac{1}{\Delta(\Delta + b)}, & \theta = \Delta^2 + b\Delta - 1, & \xi = \Delta + b \\ \Phi = \frac{1}{\Delta(\Delta - b)}, & \Theta = \Delta^2 - b\Delta - 1, & \gamma = \Delta - b \end{cases} \quad (19)$$

Also, we have used equation (19) in calculating the non-zero terms of the reduced matrix related to the first and third qubits as well as the second and third qubits.

Now, through partial tracing on the information of the second qubit, the non-zero components of the reduced density matrix related to the first and third qubits can be calculated as follows:

$$\begin{cases} \rho_{11}^{(13)}(T) = e^{(-\beta\mathcal{B})}[e^{(-2\beta\mathcal{B})} + b^2(\frac{1}{\Delta})^2 + \xi^2\Omega^2e^{(-2\beta\Delta)} + \gamma^2\Phi^2e^{(2\beta\Delta)}] \\ \rho_{22}^{(13)}(T) = \cosh(\beta\mathcal{B})[2(\frac{1}{\Delta})^2 + 2\theta^2\Omega^2e^{(-2\beta\Delta)} + 2\Theta^2\Phi^2e^{(2\beta\Delta)}] \\ \rho_{23}^{(13)}(T) = \cosh(\beta\mathcal{B})[2(\frac{1}{\Delta})^2 + 2\theta\Omega^2e^{(-2\beta\Delta)} + 2\Theta\Phi^2e^{(2\beta\Delta)}] \\ \rho_{32}^{(13)}(T) = \cosh(\beta\mathcal{B})[2(\frac{1}{\Delta})^2 + 2\theta\Omega^2e^{(-2\beta\Delta)} + 2\Theta\Phi^2e^{(2\beta\Delta)}] \\ \rho_{33}^{(13)}(T) = \cosh(\beta\mathcal{B})[2(\frac{1}{\Delta})^2 + 2\Omega^2e^{(-2\beta\Delta)} + 2\Phi^2e^{(2\beta\Delta)}] \\ \rho_{44}^{(13)}(T) = e^{(\beta\mathcal{B})}[e^{(2\beta\mathcal{B})} + b^2(\frac{1}{\Delta})^2 + \xi^2\Omega^2e^{(-2\beta\Delta)} + \gamma^2\Phi^2e^{(2\beta\Delta)}] \end{cases} \quad (20)$$

Finally, through partial tracing on the information of the first qubit, the non-zero terms of the reduced density matrix corresponding to the second and third qubits are obtained as follows:

$$\begin{cases} \rho_{11}^{(23)}(T) = e^{(-\beta\mathcal{B})}[e^{(-2\beta\mathcal{B})} + (\frac{1}{\Delta})^2 + \theta^2\Omega^2e^{(-2\beta\Delta)} + \Theta^2\Phi^2e^{(2\beta\Delta)}] \\ \rho_{22}^{(23)}(T) = (\frac{1}{\Delta})^2(b^2e^{(-\beta\mathcal{B})} + e^{(\beta\mathcal{B})}) + \Omega^2e^{(-2\beta\mathcal{B})}(\xi^2e^{(-\beta\mathcal{B})} + \theta^2e^{(\beta\mathcal{B})}) + \Phi^2e^{(2\beta\Delta)}(\gamma^2e^{(-\beta\mathcal{B})} + \Theta^2e^{(\beta\mathcal{B})}) \\ \rho_{23}^{(23)}(T) = -2(\frac{1}{\Delta})^2b\sinh(\beta\mathcal{B}) + \xi\Omega^2e^{(-2\beta\Delta)}(e^{(-\beta\mathcal{B})} + \theta e^{(\beta\mathcal{B})}) + \gamma\Phi^2e^{(2\beta\Delta)}(e^{(-\beta\mathcal{B})} + \Theta e^{(\beta\mathcal{B})}) \\ \rho_{32}^{(23)}(T) = -2(\frac{1}{\Delta})^2b\sinh(\beta\mathcal{B}) + \xi\Omega^2e^{(-2\beta\Delta)}(e^{(-\beta\mathcal{B})} + \theta e^{(\beta\mathcal{B})}) + \gamma\Phi^2e^{(2\beta\Delta)}(e^{(-\beta\mathcal{B})} + \Theta e^{(\beta\mathcal{B})}) \\ \rho_{33}^{(23)}(T) = (\frac{1}{\Delta})^2(b^2e^{(-\beta\mathcal{B})} + b^2e^{(\beta\mathcal{B})}) + \Omega^2e^{(-2\beta\Delta)}(e^{(-\beta\mathcal{B})} + \xi^2e^{(\beta\mathcal{B})}) + \Phi^2e^{(2\beta\Delta)}(e^{(-\beta\mathcal{B})} + \gamma^2e^{(\beta\mathcal{B})}) \\ \rho_{44}^{(23)}(T) = e^{(\beta\mathcal{B})}[e^{(2\beta\mathcal{B})} + (\frac{1}{\Delta})^2 + \Omega^2e^{(-2\beta\Delta)} + \Phi^2e^{(2\beta\Delta)}] \end{cases} \quad (21)$$

In this section, we examine the amount of thermal quantum entanglement of the relevant subsystems. Thermal effects tend to destroy quantum correlations, which reduces coherence. We want to see what happens to entanglement between qubits.

Using the non-zero terms of the reduced density matrix (18), (20) and (21) as well as concurrence in equation (4), the thermal entanglement of subsystems can be calculated. In this

section, we analyze the entanglement of subsystems through diagrams according to controllable parameters T , B and b .

In figure (1), the concurrence for all three adjacent qubit pairs (12), (23) and non-adjacent (13) is drawn in terms of homogeneous magnetic field B ($b = 0$). It can be seen that with the increase of the magnetic field, the thermal entanglement increases in the negative part of the diagram, then it starts to decrease in the positive part. In fact, the diagram is symmetrical. $c(\rho_{12})$ and $c(\rho_{23})$ in red, in the indicated range, are superimposed and behave similarly to each other, as we expected. $c(\rho_{13})$ with blue color has a lower value than $c(\rho_{12})$ and $c(\rho_{23})$.

In figure (2), thermal entanglement is drawn in terms of temperature T . By examining it, we find that with increasing temperature, the entanglement reaches a maximum point and then starts to decrease. $c(\rho_{12})$ and $c(\rho_{23})$ with blue color again coincide and $c(\rho_{13})$ with red color has a lower value than $c(\rho_{12})$ and $c(\rho_{23})$.

In figure (3), the thermal entanglement is drawn according to the amount of magnetic field inhomogeneity b . We notice that by increasing the amount of magnetic heterogeneity in the negative part, first the intersection reaches a maximum point, then it reaches zero, and by moving towards the positive part, it reaches its maximum value again and then decreases. In other words, the graph is symmetrical. In this diagram, $c(\rho_{23})$, which is marked in green, has the highest amount of thermal entanglement, followed by $c(\rho_{12})$ in blue and $c(\rho_{13})$ in red.

The similarity of behavior in the entanglement of $c(\rho_{12})$ and $c(\rho_{23})$ is what we expected, and what makes the difference between these two quantum thermal entanglements is the amount of inhomogeneity of the magnetic field, b . On the other hand, the amount of thermal entanglement between non-adjacent qubits, $c(\rho_{13})$, can be influenced by changing the controllable parameters so that it takes a larger value than the entanglement of adjacent qubits.

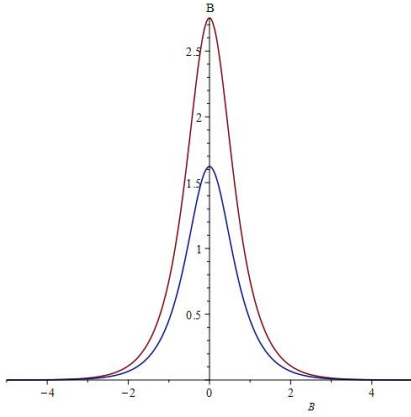


Figure 1: blue color, thermal entanglement $c(\rho_{13})$ and red color, thermal entanglement $c(\rho_{12})$ or $c(\rho_{23})$, according to the magnetic field \mathcal{B} , which is $T=1$ and $b=0$.

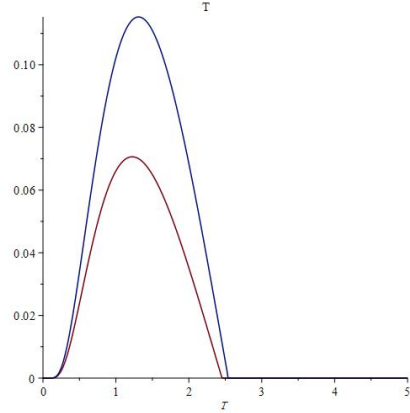


Figure 2: red color, thermal entanglement $c(\rho_{13})$ and blue color, thermal entanglement $c(\rho_{12})$ or $c(\rho_{23})$, according to temperature T , which is $\mathcal{B}=2$ and $b=0$.

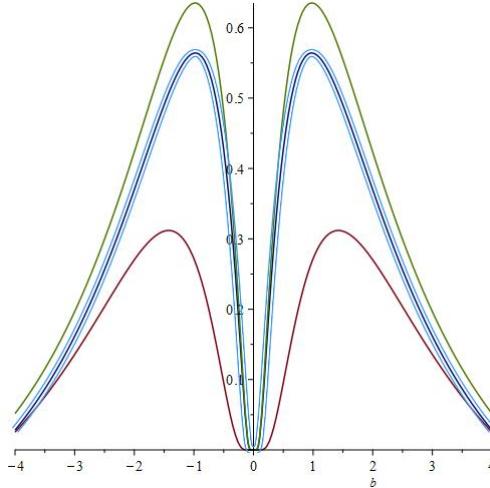


Figure 3: Red color, thermal entanglement $c(\rho_{13})$, blue color thermal entanglement $c(\rho_{12})$ and green color thermal entanglement $c(\rho_{23})$, according to the value of magnetic heterogeneity b , which is $\mathcal{B}=0$ and $T=1$.

5 Comparison of thermal entanglement and time-dependent entanglement

We know that quantum systems interact with their surroundings, which causes their incoherence. One of the solutions is to change the Schrödinger equation in such a way that this coherence is automatically destroyed with the evolution of the quantum system. This is called the inherent asymmetry effect. The intrinsic coherence is checked by the Markov approximation. In reference [44], the three-qubit spin chain with this type of inherent inhomogeneity is considered and the changes in the entanglement between pairs of qubits are investigated. The time evolution of the density operator for our desired system is as follows:

$$\rho(t) = \sum_{m,n} \exp\left[-\frac{\gamma t}{2}(E_m - E_n)^2 - i(E_m - E_n)t\right] \langle \psi_m | \rho(0) | \psi_n \rangle | \psi_m \rangle \langle \psi_n | \quad (22)$$

γ in the above equation is the intrinsic decoherence rate, which is written based on the eigenvalues and eigenvectors given in equations (14) and (15). Equations (14), (15) and (22) are used to calculate the density matrix, and also equation (4) is used to calculate the time entanglement, and these calculations are done in reference [15].

If we examine the intersection in terms of time changes, we will find that it decreases in an oscillatory manner as time increases. Also, with the increase of the magnetic field, the intersection increases and then decreases and repeats this behavior. In fact, for the first and second qubits, the magnetic field \mathcal{B} can contribute to the amount of field inhomogeneity to increase the time entanglement. Finally, temporal entanglement may increase and then decrease with increasing magnetic field inhomogeneity. By comparing, we can find similarities between thermal and temporal entanglement in the behavior of the system that changes according to the magnetic field \mathcal{B} and of inhomogeneity of the magnetic field b .

Also, by controlling the magnetic field and its related inhomogeneity, both entanglements can be controlled. In addition, in time crossing, we notice that the non-uniform magnetic

field can increase the crossing $c(\rho_{13})$ to a great extent, which is not possible in the other two cases. Also, the magnetic field can contribute to the amount of inhomogeneity of the magnetic field, which is true for the intersection of the first and second qubits. Similarly, in thermal quantum entanglement, we found that $c(\rho_{13})$ can be increased by changing the variable parameters such as the magnetic field and the amount of field inhomogeneity and reach a larger value than the other two cases. In the general case of time crossing, the inhomogeneity magnetic field is more useful for $c(\rho_{13})$.

6 Trace distance discord

In order to check the trace discord between adjacent and non-adjacent qubits in the studied three-spin chain, there is a need for reduced density matrices that were previously calculated in relations (18), (20) and (21) and using relations (8), (9) and (10) are non-vanishing components and the discord trace for the first and second qubit is as follows.

$$\left\{ \begin{array}{l} R_{03}^{(12)} = 1 - 2\left[\left(\frac{1}{\Delta}\right)^2(b^2e^{-\beta\mathcal{B}} + e^{2\beta\mathcal{B}}) + \Omega^2e^{-2\beta\Delta}(\xi^2e^{-\beta\mathcal{B}} + \theta^2e^{\beta\mathcal{B}} + e^{\beta\mathcal{B}}) \right. \\ \quad \left. + \Phi^2e^{2\beta\Delta}(\gamma^2e^{-\beta\mathcal{B}} + \Theta^2e^{\beta\mathcal{B}} + e^{\beta\mathcal{B}})\right], \\ R_{11}^{(12)} = 2| - 2\left(\frac{1}{\Delta}\right)^2bsinh(\beta\mathcal{B}) + \xi\Omega^2e^{-2\beta\Delta}(\theta e^{\beta\mathcal{B}} + e^{-\beta\mathcal{B}}) \\ \quad + \gamma\Phi^2e^{2\beta\Delta}(\Theta e^{\beta\mathcal{B}} + e^{-\beta\mathcal{B}})|, \\ R_{30}^{(12)} = 1 - 2\left[\left(\frac{1}{\Delta}\right)^2(2cosh(\beta\mathcal{B}) + b^2e^{\beta\mathcal{B}}) + \Omega^2e^{-2\beta\Delta}(2cosh(\beta\mathcal{B}) + \xi^2e^{\beta\mathcal{B}}) \right. \\ \quad \left. + \Phi^2e^{2\beta\Delta}(2cosh(\beta\mathcal{B}) + \gamma^2e^{\beta\mathcal{B}}) + e^{3\beta\mathcal{B}}\right], \\ R_{33}^{(12)} = 1 - 2\left[\left(\frac{1}{\Delta}\right)^2(2b^2cosh(\beta\mathcal{B}) + 2cosh(\beta\mathcal{B})) + \Omega^2e^{-2\beta\Delta}(2\xi^2cosh(\beta\mathcal{B}) + \theta^2e^{\beta\mathcal{B}} + e^{-\beta\mathcal{B}}) \right. \\ \quad \left. + \Phi^2e^{2\beta\Delta}(2\gamma^2cosh(\beta\mathcal{B}) + \Theta^2e^{\beta\mathcal{B}} + e^{-\beta\mathcal{B}})\right] \\ R_{22}^{(12)} = R_{11}^{(12)} \end{array} \right. \quad (23)$$

$$\mathcal{D}_T^{(12)}(\rho) = 2| - 2\left(\frac{1}{\Delta}\right)^2bsinh(\beta\mathcal{B}) + \xi\Omega^2e^{-2\beta\Delta}(\theta e^{\beta\mathcal{B}} + e^{-\beta\mathcal{B}}) + \gamma\Phi^2e^{2\beta\Delta}(\Theta e^{\beta\mathcal{B}} + e^{-\beta\mathcal{B}})| \quad (24)$$

The non-vanishing components and trace discord for the first and third qubits are as follows

$$\left\{ \begin{array}{l} R_{03}^{(13)} = 1 - 2[2\cosh(\beta\mathcal{B})((\frac{1}{\Delta})^2 + \Theta^2\Phi^2e^{2\beta\mathcal{B}} + \theta^2\Omega^2e^{-2\beta\mathcal{B}}) \\ \quad + e^{\beta\mathcal{B}}(b(\frac{1}{\Delta})^2 \\ \quad + \gamma^2\Phi^2e^{2\beta\Delta} + \xi^2\Omega^2e^{-2\beta\mathcal{B}} + e^{2\beta\Delta})] \\ R_{11}^{(13)} = 2|\cosh(\beta\mathcal{B})(-2(\frac{1}{\Delta})^2 + 2\Theta\Phi^2e^{2\beta\Delta} + 2\theta\Omega^2e^{-2\beta\Delta})| \\ R_{30}^{(13)} = 1 - 2[2\cosh(\beta\mathcal{B})((\frac{1}{\Delta})^2 + \Phi^2e^{2\beta\mathcal{B}} + \Omega^2e^{-2\beta\mathcal{B}}) \\ \quad + e^{\beta\mathcal{B}}(b^2(\frac{1}{\Delta})^2 + \gamma^2\Phi^2e^{2\beta\mathcal{B}} + \xi^2\Omega^2e^{-2\beta\mathcal{B}} + e^{2\beta\mathcal{B}})] \\ R_{33}^{(13)} = 1 - 2[2\cosh(\beta\mathcal{B})(2(\frac{1}{\Delta})^2 + \Theta^2\Phi^4e^{2\beta\Delta} + \theta^2\Omega^4e^{-2\beta\mathcal{B}})] \\ R_{22}^{(13)} = R_{11}^{(23)} \end{array} \right. \quad (25)$$

$$\mathcal{D}_T^{(13)}(\rho) = 2|\cosh(\beta\mathcal{B})(-2(\frac{1}{\Delta})^2 + 2\Theta\Phi^2e^{2\beta\Delta} + 2\theta\Omega^2e^{-2\beta\Delta})| \quad (26)$$

The non-vanishing components and trace discord for the second and third qubits are as follows

$$\left\{ \begin{array}{l} R_{03}^{(23)} = 1 - 2[(\frac{1}{\Delta})^2(be^{-\beta\mathcal{B}} + 2e^{\beta\mathcal{B}}) + \Omega^2e^{-2\beta\Delta}(\xi^2e^{-\beta\mathcal{B}} + (\theta^2 + 1)e^{\beta\mathcal{B}}) \\ \quad + \Phi^2e^{2\beta\Delta}(\gamma^2e^{-\beta\mathcal{B}} + (\Theta^2 + 1)e^{\beta\mathcal{B}})], \\ R_{11}^{(23)} = 2| - 2(\frac{1}{\Delta})^2b\sinh(\beta\mathcal{B}) + \xi\Omega^2e^{-2\beta\Delta}(\theta e^{\beta\mathcal{B}} + e^{-\beta\mathcal{B}}) \\ \quad + \gamma\Phi^2e^{2\beta\Delta}(\Theta e^{\beta\mathcal{B}} + e^{-\beta\mathcal{B}})|, \\ R_{30}^{(23)} = 1 - 2[(\frac{1}{\Delta})^2(2\cosh(\beta\mathcal{B}) + b^2e^{\beta\mathcal{B}}) + \Omega^2e^{-2\beta\Delta}(2\cosh(\beta\mathcal{B}) + \xi^2e^{\beta\mathcal{B}}) \\ \quad + \Phi^2e^{2\beta\Delta}(2\cosh(\beta\mathcal{B}) + \gamma^2e^{\beta\mathcal{B}})], \\ R_{33}^{(23)} = 1 - 2[2(\frac{1}{\Delta})^2\cosh(\beta\mathcal{B})(b^2 + 1) + \Omega^2e^{-2\beta\Delta}(2\xi^2\cosh(\beta\mathcal{B}) + \theta^2e^{\beta\mathcal{B}} + e^{-\beta\mathcal{B}}) \\ \quad + \Phi^2e^{2\beta\Delta}(2\gamma^2\cosh(\beta\mathcal{B}) + \Theta^2e^{\beta\mathcal{B}} + e^{-\beta\mathcal{B}})] \\ R_{22}^{(23)} = R_{11}^{(23)} \end{array} \right. \quad (27)$$

$$\mathcal{D}_T^{(23)}(\rho) = 2| - 2(\frac{1}{\Delta})^2b\sinh(\beta\mathcal{B}) + \xi\Omega^2e^{-2\beta\Delta}(\theta e^{\beta\mathcal{B}} + e^{-\beta\mathcal{B}}) + \gamma\Phi^2e^{2\beta\Delta}(\Theta e^{\beta\mathcal{B}} + e^{-\beta\mathcal{B}})| \quad (28)$$

7 Conclusion

In this study, we investigated the thermal entanglement when subjected to a inhomogeneity magnetic field for a chain of three qubits. The thermal entanglement was obtained through the given Hamiltonian and also by using mathematical calculations. In summary, in the

three cases that were investigated for thermal entanglement $c(\rho_{12})$, $c(\rho_{23})$ and $c(\rho_{13})$, thermal entanglement decreases with increasing magnetic field. For thermal entanglement in terms of temperature, as in the previous case, as the temperature increases, the quantum correlation between qubits decreases. The changes of the entanglement of the pair of qubits of the system in terms of the inhomogeneity of the magnetic field b are also the same, and we noticed that the thermal entanglement of $c(\rho_{12})$ and $c(\rho_{23})$ behaves like each other in terms of three parameters in the investigated range. And what differentiates them is the amount of inhomogeneity of the magnetic field. Also, the thermal entanglement $c(\rho_{13})$, which can be controlled by parameters that can be changed, and its value can be changed so that it increases compared to the thermal entanglement $c(\rho_{12})$ and $c(\rho_{23})$. In the investigations carried out using the Trace distance discord criterion, which has results similar to Concurrence, we see that D decreases with the increase of the three mentioned parameters, and $\mathcal{D}_T^{(12)}(\rho)$ and $\mathcal{D}_T^{(23)}(\rho)$ show a similar behavior, and the heterogeneous magnetic field is the distinguishing feature, and $\mathcal{D}_T^{(13)}(\rho)$ It has a lower value than the other two and can be increased by changing the parameters.

8 References

- [1] C.H.Bennett, G.Brassard, C.Crepeau, R. Jozsa, A.Peres, and K.Wooters, Phys. Rev. Lett. 70, 1895 (1993) [2] Luo S 2008 Phys. Rev. A 77 022301 [3] Horodecki R, Horodecki P, Horodecki M and Horodecki K 2009 Rev. Mod. Phys. [4] S. Hill and W. K. Wootters, Phys. Rev. Lett. 78, 5022 (1997). [5] A. K. Ekert, Phys. Rev. Lett. 67, 661 (1991). [6] Datta A, Shaji A and Caves C M 2008 Phys. Rev. Lett. 100 050502 [7] W. K. Wootters, Phys. Rev. Lett. 80, 2245 (1998). [8]] Osterloh A, Amico L, Falci G and Fazio R 2002 Nature [9] Henderson L and Vedral V 2001 J. Phys. A: Math. Gen [10] Y. Sun, Y. G. Chen, and H. Chen, Phys. Rev. A68, 044301 (2003). [11] L. F. Santos, G. Rigolin and C. O. Escobar, Phys. Rev. A69, 042304 (2004). [12] M. Muraao, D. Jonathan, M. B. Plenio, and V. Vedral, Phys. Rev. A59, 156 (1999). [13] G. L. Kamta and A. F. Starace, Phys. Rev. Lett. 88, 107901 (2002). [14] Rigolin G 2004 Int. J. Quantum Inf. 14 393 [15] Tomotaka Kuwahara , Naomichi Hatano . Phys. Rev. A 83, 062311 (2011) [16] Zhang G-F and Li S-S 2005 Phys. Rev. A 72 034302 [17] Asoudeh M and Karimipour V 2005 Phys. Rev. A 71 022308 [18] Guo-Feng Zhang, Shu-Shen Li. Phys. Rev. A 72, 034302 (2005) [19] Guo J-L, Mi Y-J, Zhang J and Song H-S 2011 J. Phys. B: At. Mol. Opt. Phys. 44 065504 [20] Youssef Khedif, Mohammed Daoud, El Hassan Sayouty. Phys. Scr. 94 (2019) 125106 [21] M. C. Arnesen, S. Bose, and V. Vedral, Phys. Rev. Lett. 87, 017901 (2001). [22] Onofre Rojas , M Rojas , N. S. Ananikian and S. M. de Souza. Phys. Rev. A 86, 042330 (2012) [23] X. G. Wang, Phys. Rev. A64, 012313 (2001). [24] Loss D and DiVincenzo D P 1998 Phys. Rev. A 57 120 Burkard G, Loss D and DiVincenzo D P 1999 Phys. Rev. B 59 2070 [25] Ollivier H and Zurek W H 2001 Phys. Rev. Lett [26] Debarba T, Maciel T O and Vianna R O 2012 Phys. Rev. A 86 024302 [27] aula F M, de Oliveira T R and Sarandy M S 2013 Phys. Rev. A 87 064101 [28] Luo S and Zhang Q 2004 Phys. Rev. A 69 032106 [29] Kedif Y and Daoud M 2019 Quantum Inf. Process. 18 45 [30] Ali M, Rau A R P and Alber G 2010 Phys. Rev. A 81 042105 [31] Ciccarello F, Tufarelli T and Giovannetti V 2014 New J. Phys. 16 013038 [32] Roga W, Spehner D and Illuminati F 2016 J. Phys. A: Math. Theor. 49 235301 [33] Dakić B, Vedral V and Brukner Č 2010 Phys. Rev. Lett. 105 190502 [34] Zhang G-F, Fan H, Ji A-L, Jiang Z-T, Abliz A and Liu W-M 2011 Ann. Phys. 326 2694

[35] Kedif Y and Daoud M 2018 Int. J. Mod. Phys. B 32 1850218 [36] Sha Y-T, Wang Y, Sun Z-H and Hou X-W 2018 Ann. Phys. 392 229 [37] Jin-Liang Guo , He-Shan Song. Physica A 388 (2009) 2254–2261 [38] Sun, Y., Ma, XP. & Guo, JL. Quantum Inf Process 19, 98 (2020). [39] Youssef Khedif , Mohammed Daoud. Vol. 36, No. 11, 2150074 (2021) [40] Oumennana, M., Rahman, A.U. & Mansour, M. Appl. Phys. B 128, 162 (2022) [41] A.-B. A.MohamedabA.RahmancF.M.Aldosaria 2023 Alexandria Engineering Journal 66, 861-871 [42] Paula F M, de Oliveira T R and Sarandy M S 2013 Phys. Rev. A 87 064101 [43] Bloch F 1946 Phys. Rev. 70 460 [44] Guo-Feng Zhang . Physical Review A 75, 034304 (2007)